


# Quantized-feedback hands-off control for nonlinear systems

Ankit Sachan<sup>1</sup> | Xiaogang Xiong<sup>2</sup>  | Sandeep Kumar Soni<sup>1</sup> | Shyam Kamal<sup>1</sup> | Sandip Ghosh<sup>1</sup>

<sup>1</sup> Department of Electrical Engineering Indian Institute of Technology (BHU), Varanasi, Uttar Pradesh, India

<sup>2</sup> Department of Mechanical and Automation, Harbin Institute of Technology, Shenzhen, P. R. China

## Correspondence

Xiaogang Xiong, Room 1010, Block G, HIT Campus of University Town of Shenzhen, Shenzhen 518055, China.

Email: xiongxg@hit.edu.cn

## Funding information

Shenzhen general project, Grant/Award Number: JCYJ20190806145001754; National Natural Science Foundation of China, Grant/Award Number: 11702073

## Abstract

This paper addresses a quantized feedback hands-off control for a class of nonlinear systems. Here,  $[\mathcal{K}, \mathcal{KL}]$  sector is constructed with the suitable choice of control-Lyapunov function. With adjustment policy of quantization parameters, the quantized feedback hands-off control can force the states of the nonlinear feedback system to the interior of a continuous-time  $[\mathcal{K}, \mathcal{KL}]$  sector infinite time and the Lyapunov-candidate function decreases automatically inside the designed sector. Finally, the effectiveness of the proposed method is illustrated by numerical examples.

## 1 | INTRODUCTION

The quantized control strategy is one of the leading research topics in modern engineering applications (see [1–6] and references within). Based on the coding and decoding devices, the interaction between the plant and the controller takes place. This may cause a more complex structure for controller design, but allows several merits over the classical ones such as reduced size and weight, comfortable and more economical installation and maintenance cost etc. Here, the signal quantization is done to transform a real-valued function into a piecewise constant function. Generally, it is categorized into static and dynamic quantization approaches. Static quantizer [1–3] leads to a memoryless function to obtain fixed quantizing parameters with a simplified structure for coding/decoding schemes. Meanwhile, the dynamic quantizer [4–6] adjusts the quantization levels dynamically depending upon the past behavior of coding/decoding schemes for a finite number of quantization levels.

It is eminent that the quantized control strategies refer to the nonlinear system that was active throughout the process to ensure global asymptotic stability. The present work's primary stimulation is to restrict the use of control signals such that the superfluous control signal is removed to design a hands-

off control with signal quantization. This permits the minimum assistance to the dynamical system to steer towards a stable region. The analytical approach to finding a stable region for the dynamical system is obtained via Zubov's method [7] whenever the system's energy approaches the value 1. Alternatively, in [8], a positive-definite Lyapunov function with a negative-semi definite derivative is used to decide a stable region. Based on this, Matrosov's theorem [9] pertains to a situation where a Lyapunov-candidate function establishes asymptotic stability about the equilibrium point for some bounded region and a "definitely positive" derivative of Lyapunov-candidate function for the remaining portion. Matrosov's theorem can be regarded as similar to the Lyapunov function in many instincts. As the information about the solution is not required, and there is no general/systematic method for constructing Matrosov's function similar to the Lyapunov function.

Overlooking Matrosov's theorem, the linear sector for the SISO system is outlined in [10]. Herein, the parameters to decide its boundary are computed by the algebraic Riccati equation, and a switching controller is utilized to drive the states within the linear sector neighborhood. Similarly, a nonlinear sector is designed in [11] by solving a forward integration differential Riccati equation for a time-varying nonlinear system. Although the state-dependent Riccati equation (SDRE) based

This is an open access article under the terms of the [Creative Commons Attribution](https://creativecommons.org/licenses/by/4.0/) License, which permits use, distribution and reproduction in any medium, provided the original work is properly cited.

© 2021 The Authors. *IET Control Theory & Applications* published by John Wiley & Sons Ltd on behalf of The Institution of Engineering and Technology

suboptimal control ensures local asymptotic stability by estimating an attractive region around the equilibrium point. These estimated regions provide the existence of global asymptotic stability for the closed-loop system, as cited in [12–14]. Moreover, many other publications are available for defining a region of attraction for several systems in [16–18]. All these designs involve the solution of the Riccati equation to decide its boundaries. An alternative way to decide the boundary of a nonlinear sector is via the control-Lyapunov function [15]. Next, the stability analysis of the dynamical system is refined with the comparison functions [19] to achieve the required uniformity. Using the same idea, a continuous-time  $[\mathcal{K}, \mathcal{KL}]$  sector is designed in [20] where the states monotonically decrease towards the origin. Moreover, the same idea is exploited for the discrete-time  $[\mathcal{K}, \mathcal{KL}]$  sector [21], robust  $[\mathcal{K}, \mathcal{KL}]$  sector [22], and continuous-time  $[\mathcal{K}, \mathcal{KL}]$  sector in the presence of disturbance [23]. In addition to this, some of the robust control techniques for the stabilization of nonlinear system has been explained in [24–29]. The complete state information is not always available due to the expansive cost and unavailability of the sensors. Thus, output feedback control is one of the methods reported in [32–34] for stabilizing nonlinear systems with limited information.

## 1.1 | Motivation

Quantization is the process of mapping the continuous signal into a set of discrete finite values. It introduces limit on the precision and range of value because of quantization error like rounding of the fractional part of a signal or overflow of the dynamic range of signal. The signal quantization problem for the linear/nonlinear systems is extensively studied in the literature, see [1–6]. One of the fundamental issues in the signal quantization problem is how to choose the quantizer and the quantized control strategy. A quantizer maps a real-valued function to a piecewise constant function for finite values of the subset. In the present work, we consider a recently proposed hands-off control design for nonlinear system with static quantization strategy to show the simplified structure for coding/decoding scheme in order to utilize low power micro controllers and to restrict the enormous use of information processing units in modern engineering control, which motivated us to propose a new algorithm. Thus, the quantized-feedback hands-off control is proposed to drag the system trajectory to the continuous-time  $[\mathcal{K}, \mathcal{KL}]$  sector in finite-time and goes offline for further convergence of the system trajectory for the inside of the sector to highlight the restricted use of control signal.

## 1.2 | Main contribution

In [20], a  $[\mathcal{K}, \mathcal{KL}]$  sector-based control design is presented for nonlinear system. Here, the decomposition of state-space is based on the sign-definiteness of the Lyapunov function derivative. The hands-off control law is permitted to converge the system trajectories outside of  $[\mathcal{K}, \mathcal{KL}]$  sector. However,

due to discrete-valued signal measurement and limited control field capacity, we gradually explore signal quantization. As per authors' knowledge, the newly proposed control algorithm, feedback quantization of hands-off control has not been presented in the literature. This paper presents an innovative and easy answer for signal quantization with limited control effort by proposing a quantized-feedback hands-off control to drag the state trajectory to the continuous-time  $[\mathcal{K}, \mathcal{KL}]$  sector in finite-time. For the simplicity of exposition, we check the condition of sign-definiteness of the Lyapunov-candidate function to construct a nonlinear sector. Here, the interaction between the plant and the controller is featured through a communication channel via coding/decoding devices. Then one can obtain signal quantization of the nonlinear system with a discrete-time adjustment policy of the quantizing parameter. Moreover, the decomposition of the nonlinear differential equation into quantized differential function and error dynamics can be performed via the mean-value theorem [30]. Finally, the switching controller based on On-Off logic is used to show asymptotic stability about the equilibrium point for the nonlinear system with a limited amount of control.

## 1.3 | Rest of this paper

Notations and some subsidiary definitions are provided in the remainder of this section. In Section 2, we briefly recall the mean-value theorem to divide the signal with the system description. The design of a continuous-time  $[\mathcal{K}, \mathcal{KL}]$  sector and the quantization phenomenon across its boundary are discussed in Sections 3 and 4, respectively. Section 5 allows the mathematical guarantee for quantized-feedback hands-off control to ensure global stabilization with the Lyapunov-second method. Finally, some insightful examples are shown in Section 6.

## 1.4 | Notation and some definitions

Although the paper,  $\mathbb{R}$  denotes the set of real numbers and  $\mathbb{R}^n$  denotes the column vector as  $\{\zeta = [\zeta_1, \zeta_2, \dots, \zeta_n]^T\}$ . Here,  $|\cdot|$  stands for the standard Euclidian norm of vectors as well as the induced norms of matrices. The signum function is written as  $\text{sgn}(\zeta)$  with conditions:  $\text{sgn}(\zeta) = 1$ ,  $\text{sgn}(-\zeta) = -1$  for all  $\zeta > 0$  and  $\text{sgn}(\zeta = 0) = 0$ . A function  $\varphi : \mathbb{R}_{\geq 0} \rightarrow \mathbb{R}_{\geq 0}$  is class  $\mathcal{K}$  ( $\varphi \in \mathcal{K}$ ), if it is monotonically increasing, continuous and  $\varphi(0) = 0$ ;  $\varphi \in \mathcal{K}_\infty$  if in addition,  $\varphi(s) \rightarrow \infty$  as  $s \rightarrow \infty$ . A function  $\delta : \mathbb{R}_{\geq 0} \times \mathbb{R}_{\geq 0} \rightarrow \mathbb{R}_{\geq 0}$  is class  $\mathcal{KL}$  if  $\delta(\cdot, t) \in \mathcal{K}$  for each fixed  $t > 0$  and  $\delta(s, t) \rightarrow 0$  as  $t \rightarrow \infty$  for each  $s \geq 0$ .

## 2 | PROBLEM FORMULATION AND PRELIMINARIES

Consider an input-affine nonlinear system in its standard form:

$$\dot{\zeta} = \mathcal{A}(\zeta) + \mathcal{B}(\zeta)u, \quad (1)$$

where  $\zeta \in \mathcal{Z} \subset \mathbb{R}^n$  are state vectors and  $u \in \mathbb{R}$  is control-input vector,  $\mathcal{Z}$  is an compact (closed and bounded) set with an equilibrium point  $0 \in \mathcal{Z}$ ,  $\mathcal{A} : \mathcal{Z} \rightarrow \mathbb{R}^n$  and  $\mathcal{B} : \mathcal{Z} \rightarrow \mathbb{R}^n$  are Lebesgue measurable and essentially bounded functions of suitable dimensions, and the pair  $(\mathcal{A}(\zeta), \mathcal{B}(\zeta))$  is stabilizable.

Consequently, it seems to quantize the control signal with a quantizer before implementing a quantized-feedback control law to a nonlinear system. In general, quantizer is a device which converts a real-valued function into a piecewise constant function  $x : \mathbb{R}^n \rightarrow \mathcal{X}$ , where  $\mathcal{X}$  is a finite subset of  $\mathbb{R}^n$  which leads to a finite number of quantization region  $\{\eta \in \mathbb{R}^n : x(\eta) = i, i \in \mathcal{X}\}$ . More precisely, we assume two positive real numbers  $\mathcal{N}$  and  $\Delta$  such that

$$\text{If } |\eta| \leq \mathcal{N}, \quad \text{then } |x(\eta) - \eta| \leq \Delta, \quad (2)$$

where  $\mathcal{N} > \Delta > 0$  and we refer  $\mathcal{N}$  and  $\Delta$  as the range and the quantization error of the quantizer, respectively. Here, the quantizer does not saturate and the quantization error seems to be bounded.

In the control design of the plant, the quantized measurement of one parameter family is considered [5]

$$x_\mu(\eta) := \mu x\left(\frac{\eta}{\mu}\right), \quad (3)$$

where  $\mu > 0$  is a quantization sensitivity of the quantizer, and  $x_\mu(\cdot)$  is uniform quantizer with the quantizing level  $\mu$ .

Define the quantization error

$$e_\mu(\eta) = x_\mu(\eta) - \eta, \quad (4)$$

where each element of the quantization error  $e_\mu(\eta)$  is less than or equal to the half of the quantization sensitivity  $\mu$  whenever the quantized state is in the range of quantizer such that

$$|\eta| \leq \mathcal{N}\mu \Rightarrow |e_\mu(\eta)| = |x_\mu(\eta) - \eta| \leq \Delta\mu, \quad (5)$$

where  $\Delta = \sqrt{n}/2$  and  $n$  is the dimension of the system.

However, for the quantization of nonlinear differential equation, the below-discussed lemma is utilized.

**Lemma 1** (Mean value theorem [30]). *Let there be function  $h : \mathbb{R}^n \Rightarrow \mathbb{R}^n$  to be continuously differentiable on an open and connected set  $\Lambda \subset \mathbb{R}^n$ . Let  $\zeta, w \in \Lambda$  such that the line segment  $L(\zeta, w) \subset \Lambda$  is designed for some particular direction. Then, there is a point  $\eta$  of  $L(\zeta, w)$  for that particular direction such that*

$$h(w) - h(\zeta) = \int_0^1 \frac{\partial h}{\partial \zeta}(\zeta + \sigma(w - \zeta)) d\sigma(w - \zeta). \quad (6)$$

Based on Lemma 1, a nonlinear function  $F(\zeta)$  is assumed to fictitiously divided into two signals, that is, the nonlinear signals consist of quantized signal and error dynamics as follows:

$$\begin{aligned} F(\zeta) &= F(x_\mu(\zeta)) - F(x_\mu(\zeta)) + F(\zeta) \\ &= F(x_\mu(\zeta)) - \int_0^1 \frac{\partial F}{\partial \zeta}(\zeta + \sigma(x_\mu(\zeta) - \zeta)) d\sigma(x_\mu(\zeta) - \zeta) \\ &= F(x_\mu(\zeta)) - F(e_\mu(\zeta)) \end{aligned} \quad (7)$$

$$\text{where } F(e_\mu) = \int_0^1 \frac{\partial F}{\partial \zeta}(\zeta + \sigma e_\mu) d\sigma \times e_\mu \cong Y\Delta\mu.$$

### 3 | DESIGN OF CONTINUOUS-TIME $[\mathcal{K}, \mathcal{KL}]$ SECTOR

For design, a continuous-time  $[\mathcal{K}, \mathcal{KL}]$  sector is proclaimed by the Matrosov's proof [9] where the state-space is decomposed into two mutually exclusive regions, that is, for the attractive region, the Lyapunov-candidate function derivative is negative semi-definite. For the non-attractive region, the Lyapunov-candidate function derivative is positive definite. The first region is reconsidered as a special subset to form a continuous-time  $[\mathcal{K}, \mathcal{KL}]$  sector as follows:

**Definition 1.** A continuous-time  $[\mathcal{K}, \mathcal{KL}]$  sector  $\mathfrak{N}$  for the nonlinear system (1) is defined as

$$\mathfrak{N} = \{\zeta \mid \varrho^2(\zeta) \leq \xi^2(\zeta), \quad \forall \zeta \in \mathbb{R}^n\}, \quad (8)$$

inside which a Lyapunov-candidate function  $W : \mathcal{Z} \rightarrow \mathbb{R}^n$  bounded between Lipschitz class  $\mathcal{K}_\infty$  function, that is,  $\varphi_1, \varphi_2 \in \mathcal{K}_\infty$  is defined by

$$\varphi_1(|\zeta|) \leq W(\zeta) \leq \varphi_2(|\zeta|), \quad \forall \zeta \in \mathcal{Z}, \quad (9)$$

decreases monotonically with a hands-off control law and its derivative along with the trajectories of the nonlinear system (1) inside the sector satisfies

$$\frac{d}{dt} W(\zeta) = \frac{\partial W}{\partial \zeta} \mathcal{A}(\zeta) \leq -\hat{\varphi}_3(|\zeta|), \quad \forall \zeta \in \mathfrak{N} \quad (10)$$

where  $\hat{\varphi}_3$  is a Lipschitz class  $\mathcal{K}_\infty$  function and the two nonlinear functions  $\varrho(\zeta)$  and  $\xi(\zeta)$  are defined as an explicitly dependent switching function and a square root of the difference of Lyapunov-candidate function derivative without control and with control to decide the necessity of control input, respectively, and determined as

$$\varrho(\zeta) = \Xi, \quad (11)$$

$$\xi(\zeta) = \sqrt{|\varphi_3(|\zeta|) - \hat{\varphi}_3(|\zeta|)|}. \quad (12)$$

where  $\varphi_3(|\zeta|)$  is a Lipschitz class  $\mathcal{K}_\infty$  function.

As the inequality (10) shows a certain level of negativity to achieve asymptotic stability such that  $W(\zeta) \rightarrow 0$  as  $t \rightarrow \infty$ . Then, the solution of Lyapunov-candidate function is given as

$$\frac{dW}{dt} \leq -\hat{\varphi}_3(\varphi_2^{-1}(W(\zeta))) = -\varphi(W(\zeta)),$$

where  $\varphi(\cdot) = \hat{\varphi}_3 \circ \varphi_2^{-1}(\cdot)$  and by integration, we get

$$W(\zeta(t)) \leq W(\zeta(0)) - \pi t. \tag{13}$$

Therefore, we conclude that  $W(\zeta(t)) \leq W(\zeta(0))$  and the trajectories of the nonlinear system (1) monotonically decreases inside the continuous-time  $[\mathcal{K}, \mathcal{KL}]$  sector to moves towards the origin asymptotically.

*Remark 1.* There are four nonlinear functions to configure a continuous-time  $[\mathcal{K}, \mathcal{KL}]$  sector, among which  $\varphi_3(|\zeta|)$  and  $\hat{\varphi}_3(|\zeta|)$  determine the performance of the nonlinear system with control input and without control input and  $\varrho(\zeta)$  and  $\xi(\zeta)$  are chosen to decide the shape of the nonlinear sector.

For a generalized nonlinear system, a control input is allowed to move the trajectories of the nonlinear system to drive the state vectors to the interior of a continuous-time  $[\mathcal{K}, \mathcal{KL}]$  sector and eventually towards the origin such that

$$\dot{W}(\zeta) = \frac{\partial W}{\partial \zeta} \mathcal{A}(\zeta) + \frac{\partial W}{\partial \zeta} \mathcal{B}(\zeta) u_C \leq -\varphi_3(|\zeta|), \quad \forall \zeta \in \mathfrak{N}, \tag{14}$$

and the boundary of a continuous-time  $[\mathcal{K}, \mathcal{KL}]$  sector has been designed by shifting the control signal to right hand side in (14) and a dummy control-Lyapunov function, that is,  $u_C = -\frac{1}{4}(\frac{\partial W}{\partial \zeta} \mathcal{B}(\zeta))^T$  is chosen as a control input such that

$$\begin{aligned} \dot{W}(\zeta) &= \frac{\partial W}{\partial \zeta} \mathcal{A}(\zeta) \leq -\frac{\partial W}{\partial \zeta} \mathcal{B}(\zeta) \times -\frac{1}{4} \left( \frac{\partial W}{\partial \zeta} \mathcal{B}(\zeta) \right)^T - \varphi_3(|\zeta|) \\ &= \left( \frac{1}{2} \frac{\partial W}{\partial \zeta} \mathcal{B}(\zeta) \right)^T \frac{1}{2} \frac{\partial W}{\partial \zeta} \mathcal{B}(\zeta) - \varphi_3(|\zeta|) \\ &\quad - \varphi_3(|\zeta|) + \hat{\varphi}_3(|\zeta|) - \hat{\varphi}_3(|\zeta|) \\ &= \varrho^2(\zeta) - \xi^2(\zeta) - \hat{\varphi}_3(|\zeta|). \end{aligned} \tag{15}$$

With this explanation, the various nonlinear functionals for continuous-time  $[\mathcal{K}, \mathcal{KL}]$  sector are designed as follows

$$\varrho(\zeta) = \Xi = \frac{1}{2} \frac{\partial W}{\partial \zeta} \mathcal{B}(\zeta), \tag{16}$$

$$\xi(\zeta) = \sqrt{|\varphi_3(|\zeta|) - \hat{\varphi}_3(|\zeta|)|} = (\phi \varphi_3(|\zeta|))^{1/2}, \tag{17}$$

where the positive scalar  $\phi$  satisfies  $0 < \phi < 1$  and follows the relation  $\xi^2(\zeta) = \phi \varphi_3(|\zeta|)$  and  $\hat{\varphi}_3(|\zeta|) = (1 - \phi) \varphi_3(|\zeta|)$ .

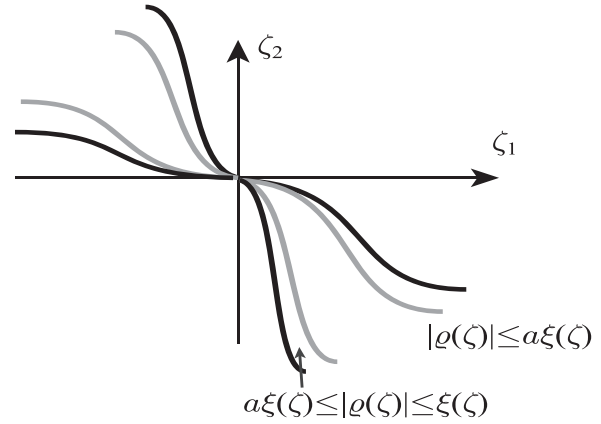


**FIGURE 1** Two-dimensional plot to represent a safety margin [31] at the boundary of a continuous-time  $[\mathcal{K}, \mathcal{KL}]$  sector

The potential chattering that appears due to switching control law is mitigated by designing a safety margin  $a$  ( $0 < a < 1$ ) [31] at the boundary of continuous-time  $[\mathcal{K}, \mathcal{KL}]$  sector as shown in Figure 1 such that an inner  $[\mathcal{K}, \mathcal{KL}]$  sector  $\mathfrak{N}_i$  and an outer  $[\mathcal{K}, \mathcal{KL}]$  sector  $\mathfrak{N}_o$  are, respectively, designed as

$$\mathfrak{N}_i = \{\zeta \mid |\varrho(\zeta)| \leq a \xi(\zeta), \quad \forall \zeta \in \mathbb{R}^n\}, \tag{18}$$

$$\mathfrak{N}_o = \{\zeta \mid a \xi(\zeta) < \varrho(\zeta) \leq \xi(\zeta), \quad \forall \zeta \in \mathbb{R}^n\}, \tag{19}$$

where one can found  $\mathfrak{N} = \mathfrak{N}_i \cup \mathfrak{N}_o$  and  $\Omega = \mathfrak{N}_i \cap \mathfrak{N}_o$ , where  $\Omega$  is the null set.

With the design of an inner  $[\mathcal{K}, \mathcal{KL}]$  sector  $\mathfrak{N}_i$  (18) and an outer  $[\mathcal{K}, \mathcal{KL}]$  sector  $\mathfrak{N}_o$  (19) as a subset of  $[\mathcal{K}, \mathcal{KL}]$  sector  $\mathfrak{N}$ , a switching function  $\chi(\varrho(\zeta), \xi(\zeta))$  that depends on  $\varrho(\zeta)$  and  $\xi(\zeta)$  is defined as

$$\chi(\varrho(\zeta), \xi(\zeta)) = \begin{cases} 0, & \zeta \in \mathfrak{N}_i, \\ \text{unchanged}, & \zeta \in \mathfrak{N}_o, \\ 1, & \zeta \in \mathbb{R}^n \setminus \mathfrak{N}. \end{cases} \tag{20}$$

The supervisor uses the switching function conditions  $\chi(\varrho(\zeta), \xi(\zeta))$  for deciding the availability of the control signal such that

- System trajectories of the nonlinear system are driven from outside to inside of continuous-time  $[\mathcal{K}, \mathcal{KL}]$  sector with the help of a control signal if the initial states are outside of continuous-time  $[\mathcal{K}, \mathcal{KL}]$  sector.
- The effect of the control signal remains unchanged for the outer  $[\mathcal{K}, \mathcal{KL}]$  sector, that is, it is active if system trajectories are moving from outside to inside of the continuous-time  $[\mathcal{K}, \mathcal{KL}]$  sector. It is inactive if system trajectories move from inner  $[\mathcal{K}, \mathcal{KL}]$  sector to outside.
- The control signal remains offline whenever the system trajectories are inside of the inner  $[\mathcal{K}, \mathcal{KL}]$  sector to save the unnecessary use of the control signal.

## 4 | QUANTIZATION PHENOMENON OVER CONTINUOUS-TIME $[\mathcal{K}, \mathcal{KL}]$ SECTOR

In the sequel, the quantization sensitivity of the quantizer  $\mu$  is adjusted across the boundary of continuous-time  $[\mathcal{K}, \mathcal{KL}]$  sector. Here, a simple adjustment policy of nonlinear function  $\varrho(\zeta)$  is discussed in Theorem below:

**Theorem 1.** Choose a constant  $\psi > 1$  and suppose that the quantization error  $e_\mu > 0$  satisfies the relation:

$$|e_\mu| \leq \frac{|\varrho(\zeta)|}{(\psi + 1)|\mathcal{Y}_\varrho|}, \quad (21)$$

then the below inequality holds

$$|\varrho(e_\mu)| \leq |\mathcal{Y}_\varrho| |e_\mu| \leq \frac{1}{\psi} |\varrho(x_\mu)|. \quad (22)$$

*Proof.* Assume the quantization error of an invariant surface as

$$|\varrho(e_\mu)| \leq |\mathcal{Y}_\varrho| |e_\mu|, \quad (23)$$

where  $|\mathcal{Y}_\varrho| \cong \left| \int_0^1 \frac{\partial \varrho}{\partial \zeta} (\zeta + \sigma e_\mu) d\sigma \right|$ . Next, the adjustment policy of the quantization error satisfies  $0 < |e_\mu| < \{|\varrho(\zeta)| / (\psi + 1) |\mathcal{Y}_\varrho|\}$ , if we illustrate the condition  $|\mathcal{Y}_\varrho| |e_\mu| \leq (1/\psi) |\varrho(x_\mu)|$  to exist.

By multiplying  $(\psi + 1) |\mathcal{Y}_\varrho|$  from both sides of (21), we get

$$|\varrho(\zeta)| \geq (\psi + 1) |\mathcal{Y}_\varrho| |e_\mu|. \quad (24)$$

By subtracting  $|\mathcal{Y}_\varrho| |e_\mu|$  from both sides, we get

$$|\varrho(\zeta)| - |\mathcal{Y}_\varrho| |e_\mu| \geq \psi |\mathcal{Y}_\varrho| |e_\mu|. \quad (25)$$

Furthermore, with the inequality (23), one can see that

$$|\varrho(\zeta)| - |\varrho(e_\mu)| \geq \psi |\mathcal{Y}_\varrho| |e_\mu|. \quad (26)$$

From the result of triangle inequality, that is,  $|p + q| \geq |p| - |q|$ ,  $\forall p, q \in \mathbb{R}^n$ , it follows

$$|\varrho(\zeta) + \varrho(e_\mu)| \geq |\varrho(\zeta)| - |\varrho(e_\mu)| \geq \psi |\mathcal{Y}_\varrho| |e_\mu|. \quad (27)$$

Utilizing the results of mean value theorem, one can see that

$$|\varrho(e_\mu)| \geq \psi |\mathcal{Y}_\varrho| |e_\mu|. \quad (28)$$

Therefore, by combining (23) and (28), we can make the statement that the inequality (21) is obtained. This completes the proof.  $\square$

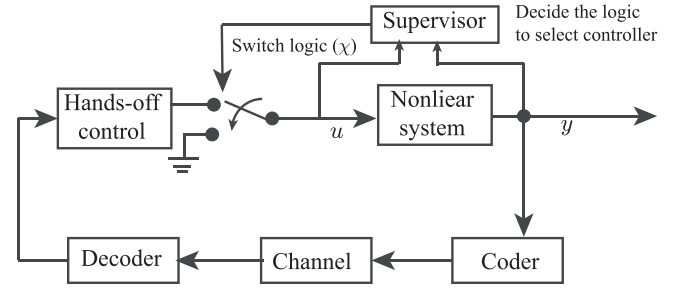


FIGURE 2 Schematic diagram of a quantized-feedback hands-off control

## 5 | DESIGN OF A QUANTIZED-FEEDBACK CONTROL LAW

In this section, the control signal's exposition is discussed for continuous-time  $[\mathcal{K}, \mathcal{KL}]$  sector. Here, a quantized-feedback hands-off control is obtained to stabilize the nonlinear system to save the redundant control effort. For this, the schematic diagram is depicted in Figure 2 for the closed-loop system with signal quantization. Here, the trajectories of the nonlinear system are firstly quantized by allowing a simplified structure of coder at one end and decoder at other end of the communication channel; then, the quantized signal is utilized to design a hands-off control as an control-input for nonlinear system. Moreover, the supervisor decides the position of the logic switch ( $\chi$ ) as discussed in Section 3 to save the unnecessary use of the control signal.

**Theorem 2.** For the nonlinear system (1), the quantized-feedback Hands-off control designed for a continuous-time  $[\mathcal{K}, \mathcal{KL}]$  sector  $\mathfrak{N}$  in (8) along with the relation  $\xi^2(\zeta) = \phi \varphi_3(|\zeta|)$  and  $\hat{\phi}_3(|\zeta|) = (1 - \phi) \varphi_3(|\zeta|)$  ( $0 < \phi < 1$ ) such that

$$u = \chi(\varrho(\zeta), \xi(\zeta))(u_1(t) + u_2(t)) \quad (29)$$

where

$$u_1(t) = - \left( \frac{\partial \Xi}{\partial \zeta} \mathcal{B}(\zeta) \right)^{-1} \frac{\partial \Xi}{\partial \zeta} \mathcal{A}(x_\mu(\zeta)) \quad (30)$$

$$u_2(t) = - \frac{\psi + 1}{\psi - 1} \left( \frac{\partial \Xi}{\partial \zeta} \mathcal{B}(\zeta) \right)^{-1} \left| \frac{\partial \Xi}{\partial \zeta} \mathcal{A}(e_\mu(\zeta)) \right| \text{sgn}(\varrho(x_\mu(\zeta))) - K \left( \frac{\partial \Xi}{\partial \zeta} \mathcal{B}(\zeta) \right)^{-1} \varrho(x_\mu(\zeta)) \quad (31)$$

and  $\chi(\varrho(\zeta), \xi(\zeta))$  is the switching function defined in (20). The trajectories of the nonlinear system (1) will be forced to move to the interior of inner  $[\mathcal{K}, \mathcal{KL}]$  sector to obtain global asymptotic stability for the sufficiently large positive constants  $\kappa_0 > 0$  and  $\psi > 1$  to satisfy the following inequality

$$2\kappa_0 \left( a^2 \phi \varphi_3(|\zeta|) - \frac{1}{\psi - 1} \varrho^\top(\zeta) \varrho(\zeta) \right) + \left( \frac{\partial \Xi}{\partial \zeta} \mathcal{A}(\zeta) \right)^\top \varrho(\zeta) + \varrho^\top(\zeta) \frac{\partial \Xi}{\partial \zeta} \mathcal{A}(\zeta) > 0, \quad (32)$$

with the controller gain condition  $K > \max(\frac{\partial \Xi}{\partial \zeta} \mathcal{B}(\zeta) / 2, \kappa_0)$ .

*Proof.* Initially, the trajectories of the nonlinear system (1) lie outside of a continuous-time  $[\mathcal{K}, \mathcal{KL}]$  sector and the quantized-feedback hands-off control in (29)–(31) is active with switching function  $\chi(\varrho(\zeta), \xi(\zeta)) = 1$  such that the movement of the trajectories is toward the inner  $[\mathcal{K}, \mathcal{KL}]$  sector.

So for the definition of quantization error in (4), the time derivative of  $\varrho^2(\zeta)$  for condition  $|\varrho(\zeta)| > a\xi(\zeta)$  follows:

$$\begin{aligned} \frac{d}{dt}\varrho^2(\zeta) &= 2\varrho(\zeta)\dot{\varrho}(\zeta) \\ &= 2\varrho(x_\mu(\zeta))\left(\frac{\partial\Xi}{\partial\zeta}\mathcal{A}(x_\mu(\zeta)) - \frac{\partial\Xi}{\partial\zeta}\mathcal{A}(e_\mu) + \frac{\partial\Xi}{\partial\zeta}\mathcal{B}(\zeta)u\right) \\ &\quad - 2\varrho(e_\mu)\left(\frac{\partial\Xi}{\partial\zeta}\mathcal{A}(x_\mu(\zeta)) - \frac{\partial\Xi}{\partial\zeta}\mathcal{A}(e_\mu) + \frac{\partial\Xi}{\partial\zeta}\mathcal{B}(\zeta)u\right). \end{aligned} \quad (33)$$

Substituting  $u = u_1 + u_2$  and  $u_1 = -\left(\frac{\partial\Xi}{\partial\zeta}\mathcal{B}(\zeta)\right)^{-1} \times \frac{\partial\Xi}{\partial\zeta}\mathcal{A}(x_\mu(\zeta))$  in above equation, then

$$\begin{aligned} \frac{d}{dt}\varrho^2(\zeta) &= 2\varrho(x_\mu(\zeta))\left(-\frac{\partial\Xi}{\partial\zeta}\mathcal{A}(e_\mu) + \frac{\partial\Xi}{\partial\zeta}\mathcal{B}(\zeta)u\right) \\ &\quad - 2\varrho(e_\mu)\left(-\frac{\partial\Xi}{\partial\zeta}\mathcal{A}(e_\mu) + \frac{\partial\Xi}{\partial\zeta}\mathcal{B}(\zeta)u\right). \end{aligned} \quad (34)$$

By the worthiness of  $|\varrho(e_\mu)| \leq \frac{1}{\psi}|\varrho(x_\mu(\zeta))|$  in (22), we get

$$\begin{aligned} \frac{d}{dt}\varrho^2(\zeta) &\leq 2\varrho(x_\mu(\zeta))\frac{\partial\Xi}{\partial\zeta}\mathcal{B}(\zeta)u_2 + 2\frac{\psi+1}{\psi}|\varrho(x_\mu(\zeta))|\left|\frac{\partial\Xi}{\partial\zeta}\mathcal{A}(e_\mu)\right| \\ &\quad + 2\frac{1}{\psi}|\varrho(x_\mu(\zeta))|\left|\frac{\partial\Xi}{\partial\zeta}\mathcal{B}(\zeta)\right||u_2|. \end{aligned} \quad (35)$$

On the other hand, with the design of  $u_2$ , we can obtain

$$\begin{aligned} &\frac{1}{\psi}\varrho(x_\mu(\zeta))\frac{\partial\Xi}{\partial\zeta}\mathcal{B}(\zeta)u_2 + \frac{1}{\psi}|\varrho(x_\mu(\zeta))|\left|\frac{\partial\Xi}{\partial\zeta}\mathcal{B}(\zeta)\right||u_2| \\ &\leq -\frac{\psi+1}{\psi(\psi-1)}\left|\frac{\partial\Xi}{\partial\zeta}\mathcal{A}(e_\mu)\right||\varrho(x_\mu(\zeta))| - \frac{K}{\psi}(\varrho(x_\mu(\zeta)))^2 \\ &\quad + \frac{\psi+1}{\psi(\psi-1)}\left|\frac{\partial\Xi}{\partial\zeta}\mathcal{A}(e_\mu)\right||\varrho(x_\mu(\zeta))| \\ &\quad + \frac{K}{\psi}\frac{\partial\Xi}{\partial\zeta}\mathcal{B}(\zeta)\left(\frac{\partial\Xi}{\partial\zeta}\mathcal{B}(\zeta)\right)^{-1}(\varrho(x_\mu(\zeta)))^2 = 0. \end{aligned} \quad (36)$$

Substituting (36) into (35), one can get

$$\begin{aligned} \frac{d}{dt}\varrho^2(\zeta) &\leq 2\frac{\psi-1}{\psi}\varrho(x_\mu)\frac{\partial\Xi}{\partial\zeta}u_2 \\ &\quad + 2\frac{\psi+1}{\psi}|\varrho(x_\mu)|\left|\frac{\partial\Xi}{\partial\zeta}\mathcal{A}(e_\mu)\right|. \end{aligned} \quad (37)$$

Furthermore, by substituting  $u_2$  in (31) in above equation, we can obtain

$$\frac{d}{dt}\varrho^2(\zeta) \leq -2K\frac{\psi-1}{\psi}(\varrho(x_\mu(\zeta)))^2. \quad (38)$$

Since  $|\varrho(x_\mu(\zeta))| = |\varrho(\zeta) + \varrho(e_\mu(\zeta))| \geq |\varrho(\zeta)| - |\varrho(e_\mu(\zeta))| \geq |\varrho(\zeta)| - \frac{1}{\psi}|\varrho(e_\mu(\zeta))|$ , we have  $|\varrho(x_\mu(\zeta))| \geq \frac{\psi}{\psi+1}|\varrho(\zeta)|$ . Then, we get

$$(\varrho(e_\mu))^2 \geq \left(\frac{\psi}{\psi+1}\right)^2(\varrho(\zeta))^2, \quad (39)$$

and by substituting the value of  $(\varrho(e_\mu(\zeta)))^2$  into (38), we get

$$\frac{d}{dt}\varrho^2(\zeta) \leq -\frac{\psi(\psi-1)}{(\psi+1)^2}K\varrho^2(\zeta), \quad (40)$$

for all  $\zeta \notin \mathfrak{N}$  and  $\chi(\varrho(\zeta), \xi(\zeta)) = 1$ . This implies that the absolute value of the switching function  $\varrho(\zeta)$  decreases for positive constants  $K > 0$  and  $\psi > 1$  and the trajectory of the nonlinear system (1) will move to the interior of inner  $[\mathcal{K}, \mathcal{KL}]$  sector  $\mathfrak{N}_i$ .

With this movement, the Lyapunov-candidate function monotonically decreases concerning time by using a quantized-feedback hands-off control (29)–(31). For this, the Lyapunov stability of the closed-loop system is analyzed by the time derivative of Lyapunov-candidate function as follows:

$$\dot{W} = \frac{\partial W}{\partial\zeta}\mathcal{A}(\zeta) + \frac{\partial W}{\partial\zeta}\mathcal{B}(\zeta)u. \quad (41)$$

For this, the trajectory of the nonlinear system in (1) is being propelled from the outside of the continuous-time  $[\mathcal{K}, \mathcal{KL}]$  sector for inequality constraint  $|\varrho(\zeta)| > a\xi(\zeta)$  and switching function  $\chi(\varrho(\zeta), \xi(\zeta)) = 1$ , such that

$$\begin{aligned} \dot{W} &= \varrho^2(\zeta) - \xi^2(\zeta) - \hat{\varphi}_3(|\zeta|) + 2\varrho(\zeta)u \\ &= \varrho^2(\zeta) - \xi^2(\zeta) + 2\varrho(\zeta)\left[-\left(\frac{\partial\Xi}{\partial\zeta}\mathcal{B}(\zeta)\right)^{-1}\frac{\partial\Xi}{\partial\zeta}\mathcal{A}(x_\mu(\zeta))\right. \\ &\quad \left.- \frac{\psi+1}{\psi-1}\left(\frac{\partial\Xi}{\partial\zeta}\mathcal{B}(\zeta)\right)^{-1}\left|\frac{\partial\Xi}{\partial\zeta}\mathcal{A}(e_\mu(\zeta))\right|\text{sgn}(\varrho(x_\mu(\zeta)))\right. \\ &\quad \left.- K\left(\frac{\partial\Xi}{\partial\zeta}\mathcal{B}(\zeta)\right)^{-1}\varrho(x_\mu(\zeta))\right] - \hat{\varphi}_3(|\zeta|). \end{aligned} \quad (42)$$

By substituting the inequality constraint  $\varrho^2(\zeta) > a^2\xi^2(\zeta)$  and the quantization error  $x_\mu(\zeta) - x = e_\mu(\zeta)$ , we get

$$\begin{aligned} \dot{W} &\leq -2\left(\frac{\partial\Xi}{\partial\zeta}\mathcal{B}(\zeta)\right)^{-1}Ka^2\xi^2(\zeta) - 2\varrho(\zeta)\left(\frac{\partial\Xi}{\partial\zeta}\mathcal{B}(\zeta)\right)^{-1} \\ &\quad \times \left(\frac{\partial\Xi}{\partial\zeta}\mathcal{A}(x_\mu(\zeta)) - \frac{\psi+1}{\psi-1}\left|\frac{\partial\Xi}{\partial\zeta}\mathcal{A}(e_\mu(\zeta))\right|\right. \\ &\quad \left.\times \text{sgn}(\varrho(x_\mu(\zeta))) - K\varrho(e_\mu(\zeta))\right) - \hat{\varphi}_3(|\zeta|). \end{aligned} \quad (43)$$

With the relation  $\xi^2(\zeta) = \phi\varphi_3(|\zeta|)$ , we get

$$\begin{aligned} \dot{W} &\leq -2\left(\frac{\partial \Xi}{\partial \zeta} g(\zeta)\right)^{-1} K a^2 \phi\varphi_3(|\zeta|) - 2\varrho(\zeta) \left(\frac{\partial \Xi}{\partial \zeta} \mathcal{B}(\zeta)\right)^{-1} \\ &\quad \times \left(\frac{\partial \Xi}{\partial \zeta} \mathcal{A}(x_\mu(\zeta)) - \frac{\psi+1}{\psi-1} \left|\frac{\partial \Xi}{\partial \zeta} \mathcal{A}(e_\mu(\zeta))\right|\right) \\ &\quad \times \text{sgn}(\varrho(x_\mu(\zeta))) - K\varrho(e_\mu(\zeta)) - \hat{\varphi}_3(|\zeta|). \end{aligned} \quad (44)$$

Noting the switching function  $\varrho(\zeta) = \varrho(x_\mu(\zeta)) - \varrho(e_\mu(\zeta))$  in (7) and by using the inequality  $|\varrho(e_\mu(\zeta))| \leq \frac{1}{\psi} |\varrho(x_\mu(\zeta))|$  in (22), we get

$$\begin{aligned} &-2\varrho(\zeta) \frac{\psi+1}{\psi-1} \left|\frac{\partial \Xi}{\partial \zeta} \mathcal{A}(e_\mu)\right| \text{sgn}(\varrho(x_\mu(\zeta))) \\ &\leq -2\frac{\psi+1}{\psi} \left|\frac{\partial \Xi}{\partial \zeta} \mathcal{A}(e_\mu)\right| |\varrho(x_\mu(\zeta))| \end{aligned} \quad (45)$$

Due to  $|\varrho(\zeta)| \leq |\varrho(x_\mu(\zeta))| + |\varrho(e_\mu(\zeta))| \leq \frac{\psi+1}{\psi} |\varrho(x_\mu(\zeta))|$ , it is easy to obtain

$$\begin{aligned} -2\varrho^\top(\zeta) \frac{\partial \Xi}{\partial \zeta} \mathcal{A}(e_\mu(\zeta)) &\leq 2|\varrho(\zeta)| \left|\frac{\partial \Xi}{\partial \zeta} \mathcal{A}(e_\mu(\zeta))\right| \\ &\leq 2\frac{\psi+1}{\psi} |\varrho(x_\mu(\zeta))| \left|\frac{\partial \Xi}{\partial \zeta} \mathcal{A}(e_\mu(\zeta))\right| \end{aligned} \quad (46)$$

And according to  $|\varrho(x_\mu(\zeta))| = |\varrho(\zeta + e_\mu(\zeta))| \leq |\varrho(\zeta)| + |\varrho(e_\mu(\zeta))| \leq |\varrho(\zeta)| + \frac{1}{\psi} |\varrho(x_\mu(\zeta))|$ , one can see that  $\frac{\psi-1}{\psi} |\varrho(x_\mu(\zeta))| \leq |\varrho(\zeta)|$ . Therefore,

$$\begin{aligned} -2\varrho^\top(\zeta) \frac{\partial \Xi}{\partial \zeta} \mathcal{A}(e_\mu(\zeta)) &\leq 2K|\varrho(\zeta)||\varrho(e_\mu(\zeta))| \\ &\leq 2K|\varrho(\zeta)| \times \frac{1}{\psi} |\varrho(x_\mu(\zeta))| \\ &\leq 2K|\varrho(\zeta)| \times \frac{1}{\psi} \times \frac{\psi}{\psi-1} |\varrho(\zeta)| \\ &= \frac{2K}{\psi-1} |\varrho(\zeta)|^2. \end{aligned} \quad (47)$$

By comparing Equations (46) and (47), we have

$$\begin{aligned} \dot{W}(\zeta) &\leq -\left(\frac{\partial \Xi}{\partial \zeta} \mathcal{B}(\zeta)\right)^{-1} \left[2K\left(a^2\phi\varphi_3(|\zeta|) - \frac{1}{\psi-1}\varrho^2(\zeta)\right) \right. \\ &\quad \left. + \left(\frac{\partial \Xi}{\partial \zeta} \mathcal{A}(\zeta)\right)^\top \varrho(\zeta) + \varrho^\top(\zeta) \frac{\partial \Xi}{\partial \zeta} \mathcal{A}(\zeta)\right] - \hat{\varphi}_3(|\zeta|). \end{aligned}$$

A sufficiently large controller gain  $K$  to fulfill the condition (32) such that

$$\dot{W} \leq -\hat{\varphi}_3(|\zeta|), \quad \forall \zeta \in \mathbb{R}^n \setminus \mathfrak{N}_i. \quad (48)$$

Once the state trajectory enters the interior of the inner  $[\mathcal{K}, \mathcal{KL}]$  sector, the control signal becomes inactive by setting the switching function  $\chi(\varrho(\zeta), \xi(\zeta))$  to be 0. For this, the constraint condition is modified as  $|\varrho(\zeta)| \leq \xi(\zeta)$  and the Lyapunov-candidate function derivative is given as,

$$\begin{aligned} \dot{W}(\zeta) &= \frac{\partial W}{\partial \zeta} \mathcal{A}(\zeta) = \varrho^2(\zeta) - \xi^2(\zeta) - \hat{\varphi}_3(|\zeta|) \\ &\leq -\hat{\varphi}_3(|\zeta|), \quad \forall \zeta \in \mathfrak{N}. \end{aligned} \quad (49)$$

As long as the trajectory of state vectors lie inside the  $[\mathcal{K}, \mathcal{KL}]$  sector, the control signal remains offline and if the trajectory reaches the boundary of the  $[\mathcal{K}, \mathcal{KL}]$  sector, the control signal becomes active and drive back to the inner  $[\mathcal{K}, \mathcal{KL}]$  sector. In this process, the quantized-feedback hands-off control (29)–(31) is allowed to monotonically decrease the energy of nonlinear system and holds the following inequality

$$\dot{W}(\zeta) \leq -\hat{\varphi}_3(|\zeta|) < 0, \quad \forall \zeta \in \mathbb{R}^n. \quad (50)$$

Thus, one can see the global stabilization for any arbitrary nonlinear system (1).  $\square$

*Remark 2.* If the quantization of the control signal is removed, then the inequality relation in (32) is reduced to  $2k_0 a^2 \phi\varphi_3(|\zeta|) + \left(\frac{\partial \Xi}{\partial \zeta} \mathcal{A}(\zeta)\right)^\top \varrho(\zeta) + \varrho^\top(\zeta) \frac{\partial \Xi}{\partial \zeta} \mathcal{A}(\zeta) > 0$  as mentioned in [20] for a continuous-time hands-off control.

*Remark 3.* If the quantized-control signal is set to be zero, the state vectors must lie somewhere to the interior of continuous-time  $[\mathcal{K}, \mathcal{KL}]$  sector.

## 6 | NUMERICAL EXAMPLES

*Example 1:* Consider an example of underwater vehicle inside the running water as given in [20] in its simplified form:

$$\dot{\nu} = -0.5\nu + \nu|\nu| + u, \quad (51)$$

where  $\nu$  is defined as the velocity of the vehicle, and the flow of the stream opposes the underwater vehicle because the friction is noted as  $-0.5\nu$ . The drag force  $\nu|\nu|$  allows non-linearity in the model due to damping coefficient  $|\nu|$ , which relaxes the sign restriction. Here, the controlled thrust  $u$  is provided by a propeller to guide the motion of the underwater vehicle.

Here, the system's initial value is set at 5, and assume a positive-definite  $C^1$  Lyapunov-candidate function as  $W = \nu^2$ .

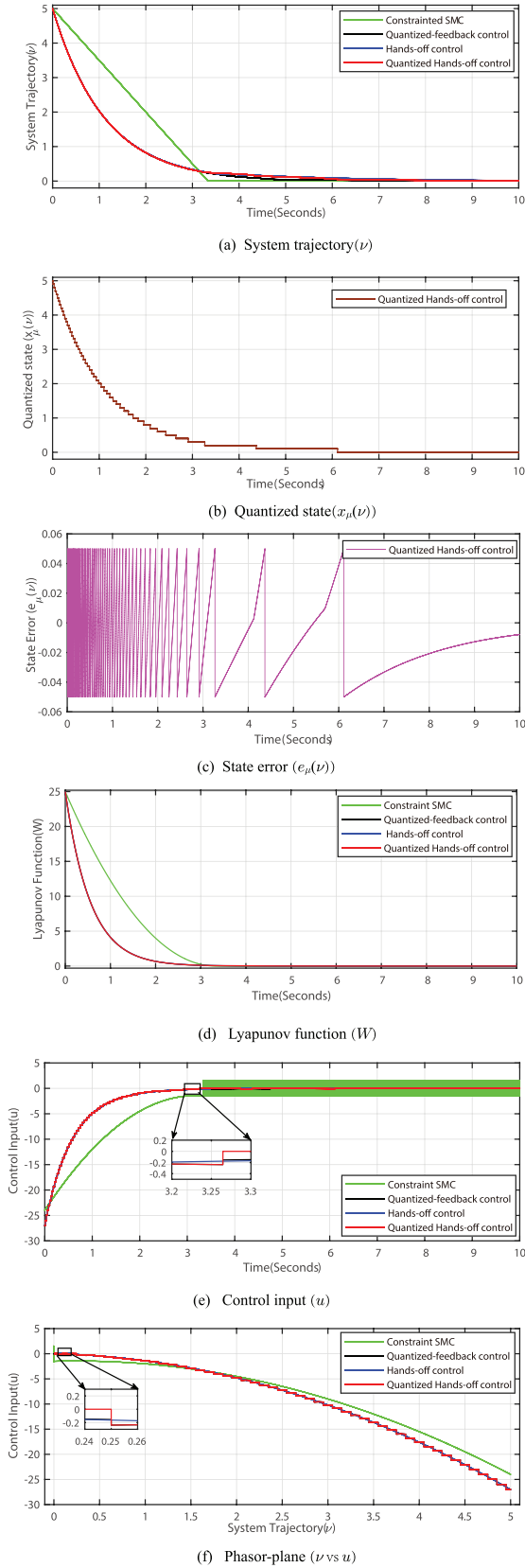


**FIGURE 3** Simulation results for an underwater vehicle inside the running water. (a) Evolution of system trajectory ( $\nu$ ). (b) Evolution of quantized state ( $x_\mu(\nu)$ ). (c) Evolution of state error ( $e_\mu(\nu)$ ). (d) Evolution of Lyapunov-candidate function ( $W$ ). (e) Evolution of control-input ( $u$ ). (f) Phasor-plane between system trajectory ( $\nu$ ) and control input ( $u$ )

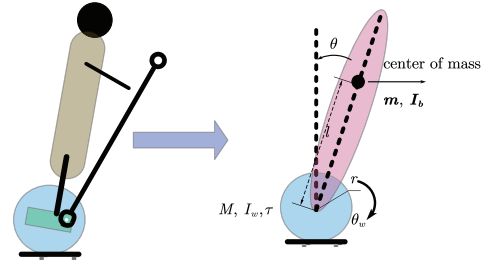


**FIGURE 4** Representation of a Segway model

Thus, to accomplish asymptotic stability, one has to design a switching controller with quantized input. The chosen control parameters for an underwater vehicle inside the running water are  $\phi = 0.8$ ,  $a = 0.9$ ,  $K = 1$  and  $\psi = 10$ . For simulation, the quantization parameter is adapted to a value of 0.1 to show a piecewise constant form, and this allows the static adjustment of the signal to achieve asymptotic stability. Finally, the compared simulation results are presented in Figure 3 for single dimensional system, which indicates the proposed method has better results.

*Example 2:* The free-body diagram for a person standing on the Segway is depicted in Figure 4. The Segway model's base platform is fastened with two wheels, which operate independently with two DC motors. The mass on the base platform is considered a point mass with a  $L$  distance from the base. The total mass occurs by a group of rotating wheels, and the chassis and person can be represented as a point mass at a certain distance from the axle. The Lagrange's equation for the rotational motion of the underactuated Segway model is described in [35, 36] as

$$\begin{aligned} m_1 \ddot{\theta}_w + m_2 \ddot{\theta} \cos(\theta) &= u + m_2 \dot{\theta}^2 \sin(\theta), \\ m_2 \ddot{\theta}_w \cos(\theta) + m_3 \ddot{\theta} &= -u + F \sin(\theta), \end{aligned} \quad (52)$$

where parameters

$$\begin{cases} m_1 = (m_b + m_w)R^2 + I_w \\ m_2 = m_b l R \\ m_3 = m_b l^2 + I_b \\ F = m_b g l \end{cases}$$

Here, the inclination and translational motion of the body are represented as  $\theta$  and  $\theta_w$ , respectively. The control torque applied to the wheels is denoted as  $u$ . However, the numerical values of the design parameter of the Segway model are given in Table 1. For the purpose of control design, (26) can be rewritten as:

$$M_1 \dot{\theta}_w + M_2 \dot{\theta} = F \sin \theta + m_2 \dot{\theta}^2 \sin \theta, \quad (53)$$

with parameters  $M_1 = m_1 + m_2 \cos \theta$  and  $M_2 = m_3 + m_2 \cos \theta$ . In order to make the state model of the Segway in chain-of-integrator form, we define  $z_1 = \theta$  and  $z_2 = \dot{\theta}$  such

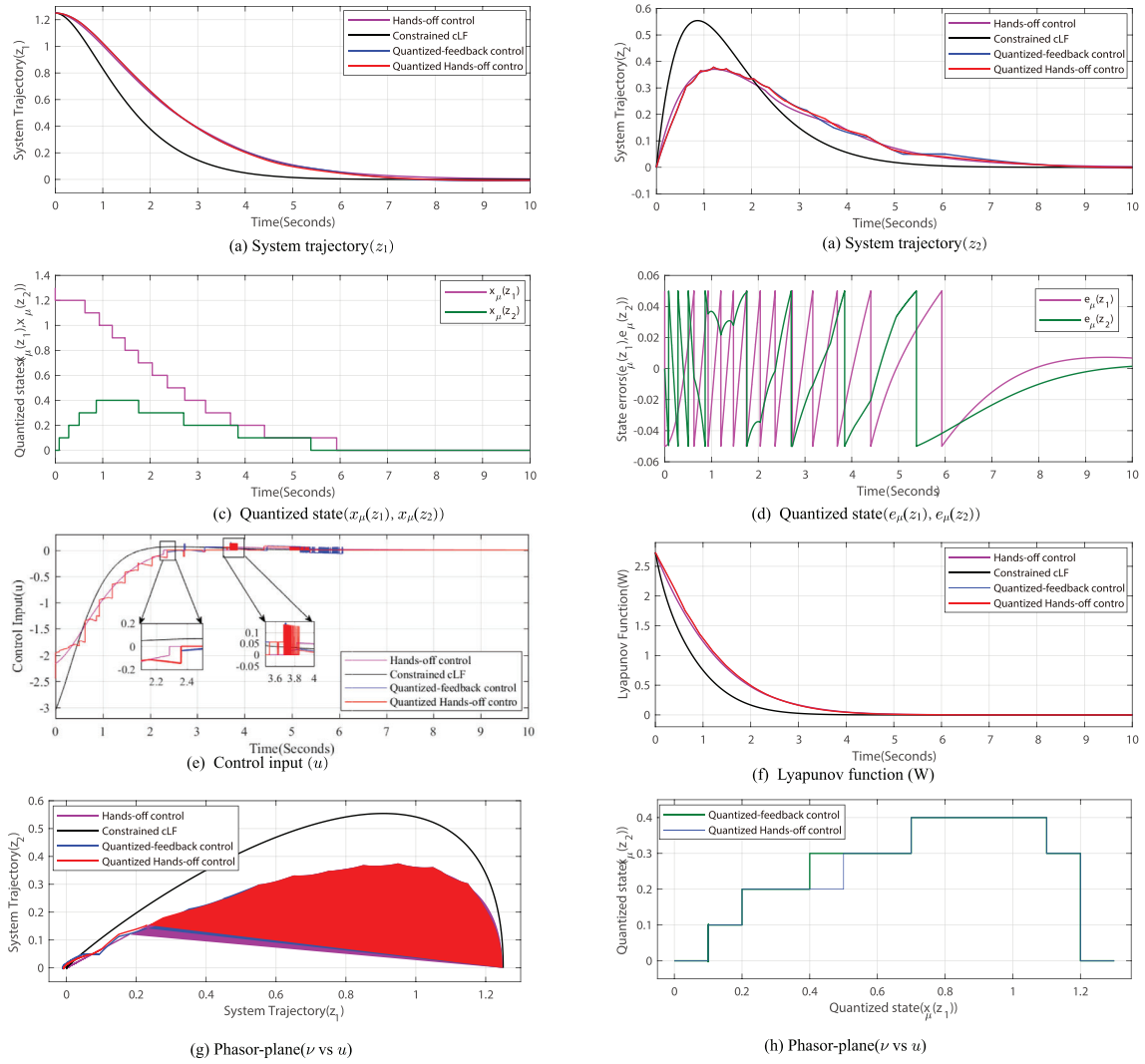


**FIGURE 5** Simulation results for a Segway model. (a) Evolution of system trajectory  $(z_1)$ . (b) Evolution of system trajectory  $(z_2)$ . (c) Evolution of quantized states  $(x_\mu(z_1), x_\mu(z_2))$ . (d) Evolution of state errors  $(e_\mu(z_1), e_\mu(z_2))$ . (e) Evolution of control-input  $(u)$ . (f) Evolution of Lyapunov-candidate function  $(W)$ . (g) Phasor-plane between the system trajectories  $(z_1)$  vs.  $(z_2)$ . (h) Phasor-plane between the quantized states  $(x_\mu(z_1))$  vs.  $(x_\mu(z_2))$

**TABLE 1** Parameter Specifications of a Segway model

Description	Symbol	Value	Unit
Radius of the wheel	$R$	0.2	m
Length between axle wheel and gravity of the body center	$l$	1.7	m
Mass of the wheel	$m_w$	3.5	kg
Mass of the person body	$m_b$	85	kg
Moment of inertia of the wheel	$I_w$	0.07	kg.m <sup>2</sup>
Moment of inertia of the person body	$I_b$	68.98	kg.m <sup>2</sup>
Gravitational constant	$g$	9.8	m/s <sup>2</sup>

that

$$\begin{aligned} \dot{z}_1 &= z_2, \\ \dot{z}_2 &= f(z_1, z_2) + g(z_1)u, \end{aligned} \quad (54)$$

where

$$\begin{cases} f(z_1, z_2) = \frac{m_2 - (m_2 * L)^2 \cos(z_1) \sin(z_1) + m_1 F \sin(z_1)}{\tilde{M}(z_1)} \\ g(z_1) = -\frac{M_1(z_1)}{\tilde{M}(z_1)} \\ \tilde{M}(z_1) = m_1 m_3 - (m_2 \cos(z_1))^2 \end{cases}$$

For the above model, a Lyapunov-candidate function is selected as  $W = \frac{7}{4}z_1^2 + 2z_1z_2 + \frac{3}{2}z_2^2$  to show the property of radial unboundedness. Here, the boundary of the nonlinear sector is decided by  $\frac{1}{2} \frac{\partial W}{\partial z} g(z)$  as mentioned in (16), that is,  $\vartheta(z) = z_1 + \frac{3}{2}z_2$ . However, the chosen parameters to select a quantized-feedback hands-off control designed for  $[\mathcal{K}, \mathcal{KL}]$  sector is similar to Example 1 to achieve global asymptotic stability with some restrictions given in (32). For simulation, the

quantization parameter is adjusted to a value of 0.1 to show a piecewise constant form, and this allows the static adjustment of the signal and lets the initial value for the inclination angle at  $72^\circ$  and the angular velocity is initially at zero. Finally, the compared simulation results are presented in Figure 5 for two-dimensional system, which indicates the proposed method has a better results.

## 7 | CONCLUDING REMARKS

The article addressed an incisive and concise control design for the stabilization of nonlinear systems with quantized input. For that, a quantized-feedback hands-off control is designed, which allows the discrete-time adjustment of the quantization parameter to extract the piecewise constant form. Also, the design of continuous-time  $[\mathcal{K}, \mathcal{KL}]$  sector is performed with the results of Matrosov's theorem, that is, the sign-definiteness of Lyapunov-candidate function derivative. Thus, the proposed controlled force the nonlinear system's trajectories go into the interior of continuous-time sector  $[\mathcal{K}, \mathcal{KL}]$  to guarantee asymptotic stability about the origin with state quantization. Finally, some insightful examples are discussed to demonstrate the validity of the proposed approach.

## ACKNOWLEDGEMENTS

This work is partially supported by National Natural Science Foundation of China (NO. 11702073) and Shenzhen General Project (No. JCYJ20190806145001754).

## PERMISSION STATEMENT TO REPRODUCE THE MATERIALS FROM THE OTHER SOURCES

None

## ORCID

Xiangang Xiong  <https://orcid.org/0000-0002-6469-5281>

## REFERENCES

1. Elia, N., Mitter, S.K.: Stabilization of linear systems with limited information. *IEEE Trans. Autom. Control* 46(9), 1384–1400 (2001)
2. Fu, M., de Souza, C.E.: State estimation for linear discrete-time systems using quantized measurements. *Automatica* 45(12), 2937–2945 (2009)
3. Ceragioli, F., Persis, C.D.: Discontinuous stabilization of nonlinear systems: quantized and switching controls. *Syst. Control Lett.* 56(7-8), 461–473 (2007)
4. Brockett, R.W., Liberzon, D.: Quantized feedback stabilization of linear systems. *IEEE Trans. Autom. Control* 45(7), 1279–1289 (2000)
5. Kameneva, T., Nešić, D.: Robustness of quantized control systems with mismatch between coder/decoder initializations. *Automatica* 45(3), 817–822 (2009)
6. Ren, W., Xiong, J.: Tracking control of nonlinear networked and quantized control systems with communication delays. *IEEE Trans. Autom. Control* (2019). <https://doi.org/10.1109/TAC.2019.2949102>
7. Vannelli, A., Vidyasagar, M.: Maximal Lyapunov functions and domains of attraction for autonomous nonlinear systems. *Automatica* 21(1), 69–80 (1985)
8. Jurdjevic, V., Quinn, J.P.: Controllability and stability. *J. Differ. Equations* 28(3), 381–389 (1978)
9. Matrosov, V.: On the stability of motion. *J. Appl. Math. Mech.* 26(5), 1337–1353 (1962)
10. Furuta, K., Pan, Y.: Variable structure control with sliding sector. *Automatica* 36(2), 211–228 (2000)
11. Pan, Y., et al.: Design of variable structure control system with nonlinear time-varying sliding sector. *IEEE Trans. on Auto. Control* 54(8), 1981–1986 (2009)
12. Langson, W., Alleyne, A.: A stability result with application to nonlinear regulation. *J. Dyn. Syst. Measur. Control* 124(3), 452–456 (2002)
13. Copur, H.E., et al.: An update algorithm design using moving region of attraction for SDRE based control law applied to a laboratory helicopter. *J. Franklin Inst.* 356(15), 8388–8413 (2019). <https://doi.org/10.1016/j.jfranklin.2019.08.007>
14. Lin, L.G., Xin, M.: Alternative SDRE scheme for planar systems. *IEEE Trans. Circuits Syst. II Express Briefs* 66(6), 998–1002 (2019)
15. Freeman, R., Kokotovic, P.V.: *Robust Nonlinear Control Design: State-Space and Lyapunov Techniques*. Springer Science & Business Media, New York (2008)
16. Balochian, S.: On the stabilization of linear time invariant fractional order commensurate switched systems. *Asian J. Control* 17(1), 133–141 (2015)
17. Zhao, X., et al.: State-dependent switching control of switched positive fractional-order systems. *ISA Trans.* 62, 103–108 (2016)
18. Ozcan, S., et al.: Nonlinear sliding sector design for multi-input systems with application to helicopter control. *Int. J. Robust Nonlinear Control* 30(6), 2248–2291 (2020)
19. Kellett, C.M.: A compendium of comparison function results. *Math. Control Sig. Syst.* 26(3), 339 (2014)
20. Sachan, A., et al.: A  $[\mathcal{K}, \mathcal{KL}]$  sector based control design for nonlinear system. *ISA Trans.* 89, 77–83 (2019)
21. Sachan, A., et al.: Discrete-time  $[\mathcal{K}, \mathcal{KL}]$  sector based hands-off control for nonlinear system. *Int. J. Robust Nonlinear Control* 30(6), 2443–2460 (2019). <https://doi.org/10.1002/rnc.4888>
22. Sachan, A., et al.: A robust  $[\mathcal{K}, \mathcal{KL}]$  sector for nonlinear system. *IEEE Trans. Circuits Syst. II Express Briefs* 67(11), 2547–2551 (2019). <https://doi.org/10.1109/TCSII.2019.2957082>
23. Sachan, A., et al.: A robustness consideration in continuous-time  $[\mathcal{K}, \mathcal{KL}]$  sector for nonlinear system. *IEEE Access* 7, 30628–30636 (2019)
24. Fei, J., Feng, Z.: Fractional-order finite-time super-twisting sliding mode control of micro gyroscope based on double-loop fuzzy neural network. *IEEE Trans. Syst. Man Cybern. Syst.* (2020). <https://doi.org/10.1109/TSMC.2020.2979979>
25. Sachan, A., et al.: Integral sliding mode for nonlinear system: A control-lyapunov function approach. In: *Advances in Machine Learning and Computational Intelligence*, pp. 813–823. Springer, Singapore (2021)
26. Fei, J., Chen, Y.: Fuzzy double hidden layer recurrent neural terminal sliding mode control of single-phase active power filter. *IEEE Trans. Fuzzy Syst.* (2020). <https://doi.org/10.1109/TFUZZ.2020.3012760>
27. Fei, J., Chen, Y.: Dynamic terminal sliding-mode control for single-phase active power filter using new feedback recurrent neural network. *IEEE Trans. Power Electron.* 35(9), 9904–9922 (2020)
28. Sachan, A., et al.: Stabilization of uncertain nonlinear systems via immersion and invariance based sliding mode control. In: *15th International Workshop on Variable Structure Systems*, pp. 79–84. IEEE, Piscataway (2018)
29. Fei, J., Wang, H.: Experimental investigation of recurrent neural network fractional-order sliding mode control of active power filter. *IEEE Trans. Circuits Syst. II Express Briefs* 67(11), 2522–2526 (2020)
30. Fikhtengol'ts, G.M.: *The Fundamentals of Mathematical Analysis*. Elsevier, Oxford (2014)
31. Kachroo, P., Tomizuka, M.: Chattering reduction and error convergence in the sliding-mode control of a class of nonlinear systems. *IEEE Trans. Autom. Control* 41(7), 1063–1068 (1996)

32. Zhai, J., Karimi, H.R.: Universal adaptive control for uncertain nonlinear systems via output feedback. *Inf. Sci.* 500, 140–155 (2019)
33. Zhai, J.: Dynamic output-feedback control for nonlinear time-delay systems and applications to chemical reactor systems. *IEEE Trans. Circuits Syst. II Express Briefs* 66(11), 1845–1849 (2019)
34. Soni, S.K., et al.: Delayed output feedback sliding mode control for uncertain non-linear systems. *IET Control Theory Appl.* 14(15) 2106–2115 (2020)
35. Kim, B.W., Park, B.S.: Robust control for the Segway with unknown control coefficient and model uncertainties. *Sensors* 16(7), 1–11 (2016)
36. Goyal, J.K., et al.: Higher order sliding mode control-based finite-time constrained stabilization. *IEEE Trans. Circuits Syst. II Express Briefs* 67(2), 295–299 (2019)

**How to cite this article:** Sachan A, Xiong X, Soni SK, Kamal S, Ghosh S. Quantized-feedback hands-off control for nonlinear systems. *IET Control Theory Appl.* 2021;15:1364–1374.  
<https://doi.org/10.1049/cth2.12128>